

Observational constraints on the growth index parameters in $f(Q)$ gravity

Dalale Mhamdi^{1,*}, Safae Dahmani^{1,†}, Amine Bouali^{1,2,‡}, Imad El Bojaddaini^{1,§}, and Taoufik Ouali^{1,¶}

¹Laboratory of Physics of Matter and Radiations,

Mohammed I University, BP 717, Oujda, Morocco,

²Higher School of Education and Training, Mohammed I University, BP 717, Oujda, Morocco

(Dated: August 23, 2024)

In this study, we analyse constraints on the growth index of matter perturbations, γ , within the framework of $f(Q)$ gravity, using recent cosmological observations, at the background and the perturbation levels, including Pantheon⁺, Cosmic Chronometer (CC), and Redshift Space Distortion (RSD) datasets. Our analysis focuses on quantifying the distortion parameter, which measures the deviation of the $f(Q)$ gravity model from the concordance Λ CDM cosmology at the background level. Specifically, we investigate two cases of the growth index parameter: a constant γ and a time-varying $\gamma(z)$. We investigate various parametrizations of the growth index γ , expressed as $\gamma = \gamma_0 + \gamma_1 y(z)$, where the function $y(z)$ assumes different forms, including constant (Γ_0), Taylor expansion around $z = 0$ (Γ_1), Taylor expansion around the scale factor (Γ_2), and an exponential form (Γ_3). By employing the Akaike Information Criterion and Bayesian Information Criterion, we find that the combined Pantheon⁺ + CC + RSD datasets impose stringent constraints on the value of the growth index. For the Γ_0 model, our results indicate that within the concordance Λ CDM model, γ is constrained to 0.545 ± 0.096 , showing strong agreement with the theoretical expectation of $\gamma_\Lambda = \frac{6}{11}$. However, within the framework of $f(Q)$ gravity, we observe $\gamma = 0.571_{-0.110}^{+0.095}$, slightly exceeding the Λ CDM value by 4.66%. Furthermore, when considering a time-varying growth index, our analysis reveals that the range of γ_0 spans from 0.596 to 0.62 across the Γ_{1-3} models. Finally, we compare the obtained results for the growth index parameters within $f(Q)$ with those from previous studies on modified gravity theories, such as $f(R)$ and $f(T)$.

Keywords: $f(Q)$ gravity, growth index, MCMC

CONTENTS

I. Introduction	1
II. $f(Q)$ framework	2
III. Linear matter perturbations	4
IV. Statistical analysis	5
A. Background data	5
B. Perturbation data	7
C. Information criteria	7
V. Results and discussions	9
A. Constant growth index	9
1. Γ_0 parametrization model	9
B. Time varying growth index	11
1. Γ_1 parametrization model	11
2. Γ_2 parametrization model	12
3. Γ_3 parametrization model	12
VI. Conclusion	13
References	13

I. INTRODUCTION

The prevailing cosmological paradigm, described by the cosmological constant, Λ , and the Cold Dark Matter (abbreviated as Λ CDM), has provided a remarkably successful framework for understanding a wide range of cosmological phenomena. From the intricate patterns imprinted on the Cosmic Microwave Background (CMB) radiation [1, 2] to the vast web of galaxies and galaxy clusters, Λ CDM accurately describes the large-scale structure formation [3, 4]. Furthermore, Λ CDM incorporates seamlessly the concept of cosmic expansion [5–7], elucidating the accelerated rate driven by dark energy, denoted by Λ .

However, despite its successes, the Λ CDM model is not without its challenges. Chief among these are coincidence [8, 9] and hierarchical [10, 11] issues. Additionally, cosmological tension such as the Hubble tension may question the credibility of Λ CDM as a standard model. This persistent discrepancy between the values of the Hubble constant derived from early and late Universe observations has become a focal point of debate within the cosmological community, for more detail on this issue, we refer the reader to [12]. Previous works of the authors of this paper have delved into this tension problem, such as the study of H_0 tension within a dynamical dark energy model [13], and the investigations of the influence of neutrino properties [14]. To address the phenomenon of accelerated expansion, scientists have introduced an exotic form of energy density within the framework of

* dalale.mhamdi@ump.ac.ma

† dahmani.safae.1026@gmail.com

‡ a1.bouali@ump.ac.ma

§ i.elbojaddaini@ump.ac.ma

¶ t.ouali@ump.ac.ma

general relativity, dubbed dark energy (DE). This has prompted the development of various models, including quintessence [15, 16], phantom [17, 18], and holography [19–21]. These approaches present intriguing avenues for reconciling observational data with theoretical predictions, offering new perspectives on the underlying dynamics of the Universe’s expansion and structure formation.

Another approach to explain the observed acceleration of the late-time Universe is theories of modified gravity. Among these Brans-Dicke [22–24] modified gravity theories, $f(R)$ gravity introduces modifications to Einstein’s general theory of relativity by incorporating a Lagrangian dependent on the scalar curvature R [25]. This framework has demonstrated success in accounting for the Universe’s accelerating expansion without invoking the concept of dark energy. Additionally, the Teleparallel Equivalent to General Relativity (TEGR) theory, extended to $f(T)$ gravity, proposes an alternative description of gravity based on torsion instead of curvature [26]. However, challenges such as violations of local Lorentz invariance have been raised in TEGR gravity. Another intriguing avenue is Symmetric Teleparallel Gravity extended to $f(Q)$ which uses non-metricity Q [27]. The $f(Q)$ modified theory of gravity has recently been extensively studied in several scenarios [27–30] (see also the recent Review on $f(Q)$ gravity in [31]). In addition, it was successfully confronted with various observational data, such as the supernovae type Ia, CMB, baryonic acoustic oscillations, growth data, and Redshift Space Distortion [32–36].

In this context, understanding the growth of cosmic structures, such as galaxies and galaxy clusters, takes on heightened significance. The growth rate of these structures, quantified by the growth index, serves as a sensitive probe of cosmological models and theories of gravity [37, 38]. This article specifically aims to investigate the growth of cosmic structures within the framework of $f(Q)$ gravity, characterized by the form $f(Q) = \alpha + \beta Q^n$, as reconstructed by Capozziello and D’Agostino [39], through Bayesian analysis employing various cosmological probes at both background and perturbation levels. For instance, in our knowledge, the growth index parameter has been constrained for modified gravity models such as $f(T)$ in [40] and $f(R)$ gravity in [41]. However, this analysis has not yet been applied to $f(Q)$ gravity. Thus, the primary aim of this study is to constrain the growth index parameter within the framework of $f(Q)$ gravity and ascertain its expression in two cases: a constant value, and a variable form expressed as $\gamma(z) = \gamma_0 + \gamma_1 y(z)$ with the following form of $y(z) = z, y(z) = z/(1+z)$, and $y(z) = ze^{-z}$. we present a comprehensive analysis of the growth index and its implications for the viability of $f(Q)$ gravity as a cosmological model. Leveraging both theoretical calculations and observational data,

we aim to shed light on the nature of gravity and its role in shaping the large-scale structure of the Universe. Furthermore, The growth index parameter provides a means to distinguish between General Relativity and modified gravity theories, prompting numerous comparative studies [40, 41]. In our previous paper [42], we have explored the same $f(Q)$ model, where the growth index parameter was constrained numerically by solving the overdensity equation. In contrast, this study takes a novel approach by considering γ as a free parameter, where we use $f = \Omega_m^\gamma$ parameterization to determine the constraints on the growth index parameters γ_0 and γ_1 . The next step is to compare our results with the Λ CDM model using statistical criteria like the Akaike Information Criterion (AIC) [43, 44] and the Bayesian Information Criterion (BIC) [45] to provides insights into the viability of $f(Q)$ gravity as a cosmological model.

The remainder of this paper is organized as follows: In section II, we provide an overview of $f(Q)$ gravity and its theoretical foundations. Section III introduces the linear matter perturbations. The observational data used for both background and perturbation are detailed in section IV. In section V, we present our results and discuss their implications for $f(Q)$ gravity models. Finally, we offer concluding remarks and directions for future research in section VI.

II. $f(Q)$ FRAMEWORK

The primary emphasis of this research lies in $f(Q)$ modified gravity models, distinguished by the presence of the non-metricity tensor [46, 47]

$$Q_{\alpha\mu\nu} = \nabla_\alpha g_{\mu\nu}, \quad (2.1)$$

where $g_{\mu\nu}$ is the metric tensor. The non-metricity scalar Q is expressed as

$$Q = -Q_{\alpha\mu\nu} P^{\alpha\mu\nu}. \quad (2.2)$$

The tensor $P^{\alpha\mu\nu}$ represents the non-metricity conjugate

$$P_{\mu\nu}^\alpha = -\frac{1}{2}L_{\mu\nu}^\alpha + \frac{1}{4}\left(Q^\alpha - \tilde{Q}^\alpha\right)g_{\mu\nu} - \frac{1}{4}\delta_{(\mu}^\alpha Q_{\nu)}, \quad (2.3)$$

with

$$L_{\mu\nu}^\alpha = \frac{1}{2}Q_{\mu\nu}^\alpha - Q_{(\mu\nu)}^\alpha, \quad (2.4)$$

and

$$Q_\alpha = g^{\mu\nu}Q_{\alpha\mu\nu}, \quad \tilde{Q}_\alpha = g^{\mu\nu}Q_{\mu\alpha\nu}. \quad (2.5)$$

The $f(Q)$ modified gravity model under study is based on the following action [27]

$$S = \int d^4x \sqrt{-g} \left[-\frac{f(Q)}{16\pi G} + \mathcal{L}_m \right]. \quad (2.6)$$

In this expression, \mathcal{L}_m denotes the Lagrangian for matter fields, G represents the Newtonian constant, $f(Q)$ is a general function of the non-metricity scalar, and g stands for the determinant of the metric tensor $g_{\alpha\beta}$. In flat space-time, the action (2.6) is equivalent to General Relativity when $f(Q) = Q$ [27]. The energy-momentum tensor can be represented as

$$T_{\mu\nu} = \frac{-2}{\sqrt{-g}} \frac{\delta(\sqrt{-g}\mathcal{L}_m)}{\delta g^{\mu\nu}}. \quad (2.7)$$

$$\frac{-2}{\sqrt{-g}} \Delta_\alpha(\sqrt{-g}f_Q P_{\mu\nu}^\alpha) - \frac{1}{2}g_{\mu\nu}f - f_Q(P_{\mu\alpha i}Q_\nu^{\alpha i} - 2Q_{\alpha i\mu}P_\nu^{\alpha i}) = T_{\mu\nu}, \quad (2.8)$$

here, $f_Q = \frac{\partial f}{\partial Q}$. The variation of the action (2.6) can be expressed as

$$\nabla_\mu \nabla_\nu (\sqrt{-g}f_Q P_\alpha^{\mu\nu}) = 0. \quad (2.9)$$

To integrate this gravitational theory into cosmology, we consider the flat Friedmann-Lemaître-Robertson-Walker (FLRW) line element, which is defined as

$$ds^2 = -dt^2 + a^2(t) [dr^2 + r^2 (d\theta^2 + \sin^2\theta d\phi^2)], \quad (2.10)$$

where $a(t)$ and t represent the scale factor, and the cosmic time, respectively. The non-metricity invariant Q as specified in Eq.(2.2), is expressed as $Q = 6H^2$, where $H = \frac{\dot{a}}{a}$ represents the Hubble function, and the dot indicates the derivative with respect to the cosmic time t . We suppose that the energy-momentum tensor is represented by a perfect fluid, i.e.

$$T_{\mu\nu} = (p + \rho) u_\mu u_\nu + P g_{\mu\nu}, \quad (2.11)$$

here, P stands for pressure, and ρ represents energy density.

Using Eqs (2.10) and (2.11), we deduce the modified Friedmann equations for $f(Q)$ gravity [27, 46]

$$6H^2 f_Q - \frac{1}{2}f = 8\pi G\rho, \quad (2.12)$$

$$(12H^2 f_{QQ} + f_Q) \dot{H} = -4\pi G(\rho + P), \quad (2.13)$$

where $f_{QQ} = \frac{\partial^2 f}{\partial Q^2}$.

In this study, we introduce a cosmological form of $f(Q)$ gravity as motivated in [39, 42]

$$f(Q) = \alpha + \beta Q^n, \quad (2.14)$$

where α , β , and n represent the free parameters of the model. This model possesses intriguing characteristics

Through the variation of the modified Einstein-Hilbert action (2.6) concerning the metric tensor $g_{\alpha\beta}$, the gravitational field equations can be represented as follows

that establish connections with both General Relativity and Λ CDM. More precisely, when $\alpha = 0$ and $\beta = n = 1$, the model aligns with General Relativity. Conversely, for $n = \beta = 1$ and $\alpha > 0$, it reflects the Λ CDM model.

We narrow our focus to the scenario where matter dominates i.e. $\rho = \rho_m$ and $P = P_m = 0$, representing a Universe consisting solely of matter without the presence of dark energy or radiation. In this context, using Eqs. (2.12), (2.13) and (2.14), the dynamical equation that describes our model can be written as follow

$$\dot{H} = -\frac{3H^2}{2n} \left(\frac{\alpha 6^{-n} H^{-2n}}{\beta - 2\beta n} + 1 \right). \quad (2.15)$$

The dynamics, described by Eq. (2.15), can be reformulated into the following expression

$$\frac{dH}{dz} - \frac{3H}{2n(z+1)} \left(\frac{\alpha 6^{-n} H^{-2n}}{\beta - 2\beta n} + 1 \right) = 0, \quad (2.16)$$

where we have used the following conversion

$$\frac{dH}{dt} = -(1+z)H(z) \frac{dH}{dz}. \quad (2.17)$$

By employing the current value of the Hubble parameter $H(z=0) = H_0$, and the normalized Hubble parameter, represented as $E^2(z) = H^2(z)/H_0^2$, we deduce the following subsequent solution of the differential equation (2.16), as follows

$$E^2(z) = \left[\left(\frac{6^{-n} 3\Omega_\alpha}{\beta - 2\beta n} + 1 \right) (z+1)^3 - \frac{6^{-n} 3\Omega_\alpha}{\beta - 2\beta n} \right]^{1/n}, \quad (2.18)$$

here, Ω_α denotes a dimensionless quantity dependent on α , n , and H_0 , given by $\Omega_\alpha = \frac{\alpha}{3H_0^{2n}}$. When $n = 1$, and by analogy with the standard model, we observe that the dimensionless energy density of matter and dark energy are equal to $\Omega_m = 1 - \frac{\Omega_\alpha}{2\beta}$ and $\Omega_\Lambda = \frac{\Omega_\alpha}{2\beta}$, respectively.

III. LINEAR MATTER PERTURBATIONS

In this section, we delve into the main points of the linear growth of matter fluctuations, exploring the incorporation of the growth index, γ , into the current analysis. Within the framework of any model concerning dark energy, including alternative theories such as modified gravity, it is widely acknowledged that at sub-horizon scales, the dark energy component is expected to be smooth. Consequently, we can consider perturbations solely within the matter component of the cosmic fluid [48]. On sub-horizon scales, the differential equation governing linear matter perturbations is expressed as [41, 49–51]

$$\ddot{\delta}_m + 2\nu H \dot{\delta}_m - 4\pi G_{\text{eff}} \rho_m \delta_m = 0. \quad (3.1)$$

Where $G_{\text{eff}} = G_N \mu(t)$, with G_N representing Newton's gravitational constant, while $\rho_m \propto a^{-3}$ represents the matter density. In summary, for standard General Relativity, $\mu = 1$, whereas in modified gravity models, $\mu \neq 1$. The solution of the aforementioned equation (3.1) is given by $\delta_m \propto D(a)$, where $D(a)$ represents the growth factor. Regardless of the gravity type, the growth rate and the growth factor of clustering are expressed through the following parameterization [52]

$$f(a) = \frac{d \ln \delta_m}{d \ln a} \simeq \Omega_m^\gamma(a), \quad (3.2)$$

and,

$$D(a) = \exp \left[\int_1^{a(z)} \frac{\Omega_m^\gamma(y)}{y} dy \right], \quad (3.3)$$

respectively. In this context, $\Omega_m(a) = \frac{\Omega_{m0}}{E^2(a)} a^{-3}$, and γ represents the growth index. The growth index plays a crucial role as it serves as a distinguishing factor between general relativity and modified gravity at cosmological scales. For instance, in the case of a constant equation of state (EoS) parameter of dark energy, ω_{de} , the growth index within the framework of general relativity is approximated by $\gamma \simeq \frac{3(\omega_{de}-1)}{6\omega_{de}-5}$ [53–56] which reduces to 6/11 for the concordance Λ CDM cosmology ($\omega_{de} = -1$). However, for $f(R)$ theory the growth index parameter takes the range of $0.40 \lesssim \gamma \lesssim 0.43$ [49, 57]. By substituting the operator $\frac{d}{dt} = H \frac{d}{d \ln a}$ and Eq. (3.2) into Eq. (3.1), we obtain the following expression

$$\frac{df}{d \ln a} + f^2 + \left(\frac{\dot{H}}{H^2} + 2 \right) f = \frac{3}{2} \mu(a) \Omega_m(a). \quad (3.4)$$

In the context of the dark energy model with an EoS parameter, ω_{de} , using Friedmann equations

$$\left(\frac{\dot{a}}{a} \right)^2 = \frac{8\pi G}{3} (\rho_m + \rho_{de}), \quad (3.5)$$

$$2 \frac{\ddot{a}}{a} + \left(\frac{\dot{a}}{a} \right)^2 = -8\pi G p_{de}, \quad (3.6)$$

and setting

$$\Omega = \frac{8\pi G \rho_m}{3H^2} = \frac{\rho_m}{\rho_m + \rho_{de}}, \quad (3.7)$$

one can show that

$$\frac{\dot{H}}{H^2} + 2 = \frac{1}{2} - \frac{3}{2} \omega_{de}(a) [1 - \Omega_m(a)]. \quad (3.8)$$

In general, the growth index may exhibit redshift dependence, $\gamma(z)$, rather than remaining constant, γ . In this context, the insertion of Eq. (3.2) into Eq. (3.4) and using

$$d\Omega = 3\Omega\omega_{de}(1 - \Omega)dx, \quad (3.9)$$

one obtains

$$-(1+z)\gamma' \ln(\Omega_m) + \Omega_m^\gamma + 3\omega_{de}(1 - \Omega_m) \left(\gamma - \frac{1}{2} \right) \frac{1}{2} = \frac{3}{2} \mu \Omega_m^{1-\gamma}, \quad (3.10)$$

where the prime signifies the derivative with respect to redshift z . Evaluating Eq (3.10) at $z = 0$ we have

$$-\gamma'(0) \ln(\Omega_{m0}) + \Omega_{m0}^{\gamma(0)} + 3\omega_{de0}(1 - \Omega_{m0}) \left[\gamma(0) - \frac{1}{2} \right] + \frac{1}{2} = \frac{3}{2} \mu_0 \Omega_{m0}^{1-\gamma(0)}. \quad (3.11)$$

In our previous work [42], we have constrained the $f(Q)$ model by solving numerically $\delta_m(a)$ from the differential equation given in Eq. (3.1) where $f(a) = \frac{d\delta(a)}{d \ln a}$. However, in this current study, the expression of growth factor f becomes described in Eq. (3.2). Here, we explore four distinct functional forms of $\gamma(z)$, where $\gamma(z) = \gamma_0 + y(z)\gamma_1$, with the expression of $y(z)$ will be specified bellow. These functional forms represent a first-order Taylor expansion around specific cosmological quantities such as the scale factor and redshift. These parameterizations are defined as follows [52, 58–62]

$$\gamma(z) = \begin{cases} \gamma_0, & \Gamma_0\text{-parametrization} \\ \gamma_0 + z\gamma_1, & \Gamma_1\text{-parametrization} \\ \gamma_0 + \frac{z}{1+z}\gamma_1, & \Gamma_2\text{-parametrization} \\ \gamma_0 + ze^{-z}\gamma_1, & \Gamma_3\text{-parametrization} \end{cases} \quad (3.12)$$

The Γ_0 model represents a constant growth index [52], with γ_1 strictly set to zero, thus $\gamma = \gamma_0$. The Γ_1 model represents an expansion around $z = 0$ [58], where $y(z) = z$. However, this parametrization is valid only at relatively low redshifts, $0 \leq z \leq 0.5$. The Γ_2 model represents an expansion around $a = 1$ [59–61], where the function y becomes $y(z) = 1 - a(z) = 1 - \frac{1}{1+z}$. At

large redshifts $z \gg 1$, we have $\gamma_\infty \simeq \gamma_0 + \gamma_1$. The last model Γ_3 represents an interpolated parametrization, with the function y reformulated as $y(z) = ze^{-z}$ [62], which smoothly connects low and high-redshift ranges. Clearly, at large redshifts $z \gg 1$, we have $\gamma_\infty \simeq \gamma_0$.

Obviously, using the Γ_{1-3} -parametrization mentioned above, which satisfies $y(z=0) = 0$ and $\gamma'(0) = \gamma_1 y'(0)$, and by using Eq. (3.11), we can express the parameter γ_1 in relation to γ_0 as follows:

$$\gamma_1 = \frac{\Omega_{m0}^{\gamma_0} + 3\omega_{de0} \left(\gamma_0 - \frac{1}{2}\right) (1 - \Omega_{m0}) - \frac{3}{2}\mu_0 \Omega_{m0}^{1-\gamma_0} + \frac{1}{2}}{y'(0) \ln \Omega_{m0}}. \quad (3.13)$$

From the above forms of $\gamma(z)$ it becomes evident that for the Γ_{1-3} parametrizations, we have $y(0) = 0$ and $y'(0) = 1$. Therefore, for the case of the Λ CDM model with $(\Omega_{m0}, \gamma_0) = (0.273, \frac{6}{11})$, Eq. (3.13) provides $\gamma_1 \simeq -0.0478$.

IV. STATISTICAL ANALYSIS

In this section, our attention is directed towards constraining the growth index parameters presented in the previous section within each $f(Q)$ parameterization models Γ_{0-3} , where γ_0 , γ_1 , and σ_8 are treated as a free parameter. We aim to constrain their value using the latest cosmological data, encompassing both background and perturbation levels. To achieve this, we employ a statistical technique known as Markov Chain Monte Carlo (MCMC) analysis [63]. The latter, constrains the model by varying them in a range of conservative priors and exploring the posteriors of the parameter space [65]. Therefore, for each parameter, we obtain its one- and two-dimensional distributions, where the one-dimensional distribution represents the parameters' posterior distribution whilst the two-dimensional one illustrates the covariance between two different parameters. We employ maximum likelihood estimation for fitting, using Python GetDist package [66]. This method maximizes the total likelihood function, \mathcal{L}_{tot} , by minimizing χ_{tot}^2 . We use several observational datasets: type Ia supernova data (Pantheon⁺, 1701 points), cosmic chronometer data (CC, 57 points), and redshift space distortion data (RSD, 20 points).

A. Background data

- **Pantheon⁺:** We include the updated Pantheon⁺ compilation supernovae dataset [67] which represents a significant advancement in our understanding of the universe's expansion history. These datasets, made of 1701 data points, are obtained from 1550 Type Ia supernovae spanning a redshift

range of $0.001 \leq z \leq 2.3$. The χ^2 function for the supernovae data sets is given by

$$\chi_{\text{Pantheon}^+}^2(P_Q, M, H_0) = \vec{D}^T \cdot (C_{\text{stat} + \text{sys}})^{-1} \cdot \vec{D}, \quad (4.1)$$

where \vec{D} is a 1701-dimensional vector and $C_{\text{stat} + \text{sys}}$ represents the covariance matrix obtained from the Pantheon⁺ sample accounting for both statistical and systematic uncertainties. The free parameters of the model are P_Q , M , and H_0 where P_Q represents the vector of parameters $P_Q = \{\Omega_\alpha, \beta, n\}$ of $f(Q)$ model, and M represents the absolute magnitude. The Pantheon+ sample has 1701SN light curves, 77 of which correspond to galaxies hosting Cepheids in the low redshift range $0.00122 \leq z \leq 0.01682$. In order to break the degeneracy between H_0 and the absolute magnitude M of Type Ia, we define the vector

$$D'_i = \begin{cases} m_i - M - \mu_i^{\text{Ceph}}, & \in \text{Cepheid hosts} \\ m_i - M - \mu_{\text{model}}(z_i), & \text{otherwise} \end{cases}$$

where μ_i^{Ceph} denotes the distance modulus associated with the Cepheid host of the i^{th} SNIa, independently measured through Cepheid calibrators. m_{Bi} and μ_{model} represent the apparent magnitudes and the predicted distance modulus, respectively. The predicted distance modulus is given according to a selected cosmological model, as follows

$$\mu_{\text{model}}(z_i, P_Q, H_0) = 5 \log_{10} D_L(z_i, P_Q, H_0) + 25, \quad (4.2)$$

where D_L denotes the luminosity distance, defined as

$$D_L(z_i, P_Q, H_0) = (1+z) \int_0^z \frac{cdz'}{H(z', P_Q, H_0)}. \quad (4.3)$$

Consequently, Eq. (4.1) can be rewritten as

$$\chi_{\text{SN}}^2 = \vec{D}'^T \cdot \mathbf{C}_{\text{Pantheon}^+}^{-1} \cdot \vec{D}' \quad (4.4)$$

- **Cosmic Chronometer data:** In Cosmic Chronometry, the Hubble parameter H values at specific redshifts z can be determined through two approaches: (i) by extracting $H(z)$ from line-of-sight BAO data [68, 69] including analysis of correlation functions of luminous red galaxies [68, 70], and (ii) by estimating $H(z)$ from differential ages Δt of galaxies using DA method [71, 72], which relies on the following relation

$$H(z) = -\frac{1}{1+z} \frac{dz}{dt} \simeq -\frac{1}{1+z} \frac{\Delta z}{\Delta t}. \quad (4.5)$$

The maximal set with 57 data points of $H(z)$ measurements spanning the redshift range $0 < z \leq 2.36$

DA method								BAO method							
z	$H(z)$	σ_H	Refs	z	$H(z)$	σ_H	Refs	z	$H(z)$	σ_H	Refs	z	$H(z)$	σ_H	Refs
0.070	69	19.6	[73]	0.4783	80.9	9	[76]	0.24	79.69	2.99	[81]	0.57	96.8	3.4	[88]
0.090	69	12	[74]	0.480	97	62	[78]	0.30	81.7	6.22	[70]	0.59	98.48	3.18	[82]
0.120	68.6	26.2	[73]	0.593	104	13	[79]	0.31	78.18	4.74	[82]	0.60	87.9	6.1	[84]
0.170	83	8	[74]	0.6797	92	8	[79]	0.34	83.8	3.66	[81]	0.61	97.3	2.1	[85]
0.1791	75	4	[79]	0.7812	105	12	[79]	0.35	82.7	9.1	[83]	0.64	98.82	2.98	[82]
0.1993	75	5	[79]	0.8754	125	17	[79]	0.36	79.94	3.38	[82]	0.73	97.3	7.0	[84]
0.200	72.9	29.6	[73]	0.880	90	40	[78]	0.38	81.5	1.9	[85]	2.30	224	8.6	[90]
0.270	77	14	[74]	0.900	117	23	[74]	0.40	82.04	2.03	[82]	2.33	224	8	[91]
0.280	88.8	36.6	[73]	1.037	154	20	[79]	0.43	86.45	3.97	[81]	2.34	222	8.5	[87]
0.3519	83	14	[79]	1.300	168	17	[74]	0.44	82.6	7.8	[84]	2.36	226	9.3	[89]
0.3802	83	13.5	[76]	1.363	160	33.6	[80]	0.44	84.81	1.83	[82]				
0.400	95	17	[74]	1.430	177	18	[74]	0.48	87.79	2.03	[82]				
0.4004	77	10.2	[76]	1.530	140	14	[79]	0.51	90.4	1.9	[85]				
0.4247	87.1	11.2	[76]	1.750	202	40	[79]	0.52	94.35	2.64	[82]				
0.4497	92.8	12.9	[76]	1.965	186.5	50.4	[80]	0.56	93.34	2.3	[82]				
0.470	89	34	[77]					0.57	87.6	7.8	[86]				

TABLE I. Hubble parameter values $H(z)$ with errors σ_H from DA and BAO methods.

z	$f\sigma_8$	Survey	Cosmological Tracer	Reference
0.02	0.398 ± 0.065	SnIa+IRAS	SN Ia + galaxies	[92]
0.025	0.39 ± 0.11	6dFGS	voids	[93]
0.067	0.423 ± 0.055	6dFGS	galaxies	[94]
0.10	0.37 ± 0.13	SDSS-veloc	DR7 galaxies	[95]
0.15	0.53 ± 0.16	SDSS-IV	eBOSS DR16 MGS	[96]
0.32	0.384 ± 0.095	BOSS-LOWZ	DR10, DR11	[97]
0.38	0.497 ± 0.045	SDSS-IV	eBOSS DR16 galaxies	[96]
0.44	0.413 ± 0.080	WiggleZ	bright emission-line galaxies	[98]
0.57	0.453 ± 0.022	CMASS-BOSS	DR12 voids+galaxies	[99]
0.59	0.488 ± 0.060	SDSS-CMASS	DR12	[100]
0.70	0.473 ± 0.041	SDSS-IV	eBOSS DR16 LRG	[96]
0.73	0.437 ± 0.072	WiggleZ	bright emission-line galaxies	[98]
0.74	0.50 ± 0.11	SDSS-IV	eBOSS DR16 voids	[101]
0.76	0.440 ± 0.040	VIPERS v7	galaxies	[102]
0.85	0.52 ± 0.10	SDSS-IV	eBOSS DR16 voids	[101]
0.978	0.379 ± 0.176	SDSS-IV	eBOSS DR14 quasars	[103]
1.05	0.280 ± 0.080	VIPERS v7	galaxies	[102]
1.40	0.482 ± 0.116	FastSound	ELG	[104]
1.48	0.30 ± 0.13	SDSS-IV	eBOSS DR16 voids	[101]
1.944	0.364 ± 0.106	SDSS-IV	eBOSS DR14 quasars	[103]

TABLE II. Data compilation of 20 $f\sigma_8(z)$ measurements.

is shown in Table I below, it includes 31 data points measured with DA method and 26 data points, obtained with BAO. The chi-square value for the cosmic chronometers is calculated according to the fol-

$$\chi_{CC}^2(P_Q, H_0) = \sum_{i=1}^{57} \left[\frac{H_{\text{obs}}(z_i) - H_{\text{th}}(z_i, P_Q, H_0)}{\sigma_H(z_i)} \right]^2, \quad (4.6)$$

where H_{obs} and H_{th} denote respectively the observed and the theoretical value of the Hubble parameter. On the other hand, $\sigma_H(z_i)$ corresponds to

the error on the observed values of the Hubble parameter $H(z)$. Throughout this paper, we denote this observation as "CC".

B. Perturbation data

- **Redshift space distortion:** One of the crucial probes of large scale structure is redshift space distortions, which provide measurements of $f\sigma_8(z)$. In galaxy redshift surveys, RSD measures the peculiar velocities of matter. The result is inferring the growth rate of cosmological perturbations. This measurement is done on a wide range of redshifts and scales. This can be obtained by measuring the ratio of the monopole and the quadrupole multipoles of the redshift space power spectrum, which depends on $\beta = f/b$. Here f is the growth rate and b is the bias the combination of $f\sigma_8(z)$ is independent of the bias factor and the bias dependence in this combination cancels out. In this study, the growth data that we use is based on the 6dFGS, SDSS-veloc, SDSS-IV, BOSS-LOWZ, CMASS-BOS, SDSS-CMAS, VIPERS v7, Fast-Sound, SnIa+IRAS, and WiggleZ galaxy surveys (see table IV). The χ_{RSD}^2 function is defined as

$$\chi_{\text{RSD}}^2(P_Q, P_\gamma, \sigma_8) = \sum_{i=1}^{20} \left(\frac{f\sigma_{8,i} - f\sigma_8(z_i, P_Q, P_\gamma, \sigma_8)}{\sigma(z_i)} \right)^2. \quad (4.7)$$

In this expression, $\sigma(z_i)$ represents the standard error associated with the observed value of $f\sigma_8$. The terms $f\sigma_{8,i}$ and $f\sigma_8(z_i)$ correspond to the observed and theoretical values of $f\sigma_8$, respectively. The theoretical $f\sigma_8$ value is given by

$$f\sigma_8(z, P_Q, P_\gamma, \sigma_8) = \sigma_8 \Omega_m(z)^{\gamma(z)} D(z, P_Q, P_\gamma, \sigma_8), \quad (4.8)$$

here, $D(z, P_Q, P_\gamma, \sigma_8)$ represents the growth factor as defined previously in Eq. (3.3). The P_γ represents the growth index parameters vector, which contains γ_0 and γ_1 , $P_\gamma = \{\gamma_0, \gamma_1\}$. The quantity $\sigma_{8,0}$ stands for the amplitude of the matter power spectrum at the scale of $8h^{-1}Mpc$ at the present time, i.e. $z = 0$. It is directly connected to the amplitude of the primordial fluctuations and is determined by the growth rate of cosmological fluctuations.

The total likelihood and chi-square functions are therefore given by

$$\mathcal{L}_{\text{tot}}(P) = \mathcal{L}_{\text{Pantheon}^+}(P_Q, H_0, M) \times \mathcal{L}_{\text{CC}}(P_Q, H_0) \times \mathcal{L}_{\text{RSD}}(P_Q, P_\gamma, \sigma_8), \quad (4.9)$$

and

$$\chi_{\text{tot}}^2(P) = \chi_{\text{Pantheon}^+}^2(P_Q, H_0, M) + \chi_{\text{CC}}^2(P_Q, H_0) + \chi_{\text{RSD}}^2(P_Q, P_\gamma, \sigma_8), \quad (4.10)$$

respectively. The vectors P_Q and P_γ contain the free parameters of the $f(Q)$ model. Nevertheless, the main parameters relevant to our study are $P_Q \equiv (\Omega_\alpha, \beta, n)$ and $P_\gamma \equiv (\gamma_0, \gamma_1)$. Note that in the case of the Λ CDM we have $P_Q \equiv \Omega_m$. Table III represents the priors of each parameter using in the MCMC analysis.

Parameter	Prior
γ_0	[0, 1]
γ_1	[-1, 1]
σ_8	[0, 2]
Ω_m	[0, 1]
Ω_α	[0, 1]
β	[0, 1]
n	[0, 2]
H_0	[40, 100]
M	[-20, -19]

TABLE III. Prior imposed on different parameters.

C. Information criteria

The secondary objective of this study is to determine the most suitable model according to observational data. The smallest χ^2 value stands for the perfect fit i.e. the most preferred model by data. However, a higher number of parameters can artificially improve the fit, leading to a smaller χ^2 , rendering it unreliable for model comparison. To address this issue, we employ the Akaike Information Criterion (AIC), a statistical tool which depends on the number of parameters, denoted as \mathcal{N} , to assess accurately the goodness of the fit of the studied models [43, 44]

$$AIC = \chi_{\text{min}}^2 + 2\mathcal{N}. \quad (4.11)$$

Additionally, we introduce the corrected Akaike Information Criterion, denoted as AIC_c , which depends on both the number of data points, represented by k (equal to 1778 in our case), and the number of parameters, denoted as \mathcal{N} , as described in [44].

$$AIC_c = \chi_{\text{min}}^2 + 2\mathcal{N} + \frac{2\mathcal{N}(\mathcal{N} + 1)}{k - \mathcal{N} - 1}, \quad (4.12)$$

similar to AIC, a model with a smaller value of AIC_c indicates that the model is better supported by the observation data. Hence, we calculate

Model	Param	γ_0	γ_1	σ_8	Ω_m	Ω_α	β	n	H_0	M
Λ CDM	Γ_0	$0.545^{+0.096}_{-0.096}$	-	$0.808^{+0.0359}_{-0.0359}$	$0.273^{+0.011}_{-0.011}$	-	-	-	$70.228^{+0.661}_{-0.661}$	$-19.363^{+0.018}_{-0.018}$
	Γ_1	$0.547^{+0.096}_{-0.096}$	$-0.0106^{+0.0014}_{-0.0014}$	$0.8071^{+0.0349}_{-0.0349}$	$0.2735^{+0.011}_{-0.011}$	-	-	-	$70.222^{+0.674}_{-0.674}$	$-19.363^{+0.018}_{-0.018}$
	Γ_2	$0.544^{+0.097}_{-0.097}$	$-0.00827^{+0.00154}_{-0.00154}$	$0.808^{+0.037}_{-0.037}$	$0.273^{+0.011}_{-0.011}$	-	-	-	$70.249^{+0.655}_{-0.655}$	$-19.362^{+0.018}_{-0.018}$
	Γ_3	$0.542^{+0.092}_{-0.092}$	$-0.047^{+0.007}_{-0.007}$	$0.802^{+0.034}_{-0.034}$	$0.273^{+0.011}_{-0.011}$	-	-	-	$70.222^{+0.651}_{-0.651}$	$-19.363^{+0.018}_{-0.018}$
$f(Q)$	Γ_0	$0.571^{+0.095}_{-0.110}$	-	$0.762^{+0.032}_{-0.037}$	-	$0.660^{+0.24}_{-0.17}$	$0.348^{+0.11}_{-0.11}$	$1.099^{+0.043}_{-0.043}$	$69.708^{+0.697}_{-0.697}$	$-19.371^{+0.018}_{-0.018}$
	Γ_1	$0.596^{+0.097}_{-0.11}$	$-0.0527^{+0.0057}_{-0.0098}$	$0.767^{+0.03}_{-0.036}$	-	$0.72^{+0.22}_{-0.12}$	$0.387^{+0.11}_{-0.089}$	$1.093^{+0.042}_{-0.042}$	$69.68^{+0.70}_{-0.70}$	$-19.372^{+0.018}_{-0.018}$
	Γ_2	$0.61^{+0.10}_{-0.11}$	$-0.22^{+0.12}_{-0.12}$	$0.764^{+0.030}_{-0.034}$	-	$0.758^{+0.20}_{-0.091}$	$0.406^{+0.11}_{-0.0075}$	$1.094^{+0.039}_{-0.044}$	$69.70^{+0.70}_{-0.70}$	$-19.371^{+0.018}_{-0.018}$
	Γ_3	$0.62^{+0.10}_{-0.12}$	$-0.359^{+0.093}_{-0.24}$	$0.760^{+0.029}_{-0.033}$	-	$0.74^{+0.22}_{-0.11}$	$0.391^{+0.11}_{-0.078}$	$1.098^{+0.042}_{-0.042}$	$69.68^{+0.69}_{-0.69}$	$-19.372^{+0.018}_{-0.018}$

TABLE IV. Summary of the mean $\pm 1\sigma$ values of the cosmological parameters using Pantheon⁺+CC+RSD datasets for both Λ CDM and $f(Q)$ models.

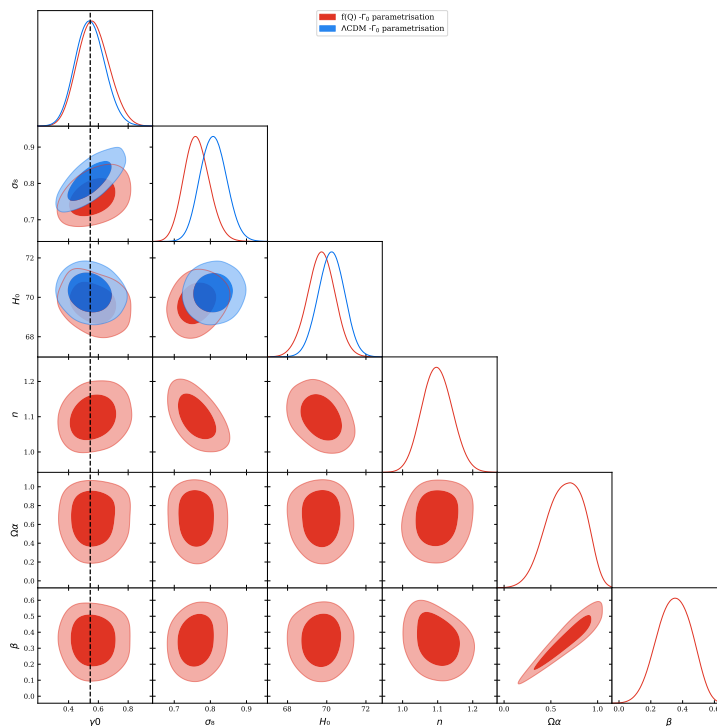


FIG. 1. This figure shows the 1σ and 2σ confidence contours and the posterior distributions obtained from the RSD+CC+Pantheon⁺ datasets for both $f(Q)$ and Λ CDM models using Γ_0 parametrization. The black dashed line represents the theoretical value of $\gamma_0 = 6/11$ for the Λ CDM model.

$$\Delta AIC = AIC_{\text{model}} - AIC_{\text{min}}. \quad (4.13)$$

The model selection rule of ΔAIC , is as follows: the models with $0 < |\Delta AIC| < 2$ have substantial support, those with $4 < |\Delta AIC| < 7$ have considerably less support, and models with $|\Delta AIC| > 10$ have essentially no support, with respect to the reference model. We also calculate the Bayesian Information Criterion (BIC), given by [45]

$$BIC = \chi_{\text{min}}^2 + \mathcal{N} \log(k), \quad (4.14)$$

where a smaller value of BIC indicates that the model is better supported by the observation data. Therefore, we calculate

$$\Delta BIC = BIC_{\text{model}} - BIC_{\text{min}}. \quad (4.15)$$

The strength of evidence against the model with the highest BIC value is as follows: for $0 \leq \Delta BIC < 2$ means that the evidence is insufficient, for $2 \leq \Delta BIC < 6$, indicates that there is a positive evidence, for $6 \leq \Delta BIC < 10$ indicates a solid evidence.

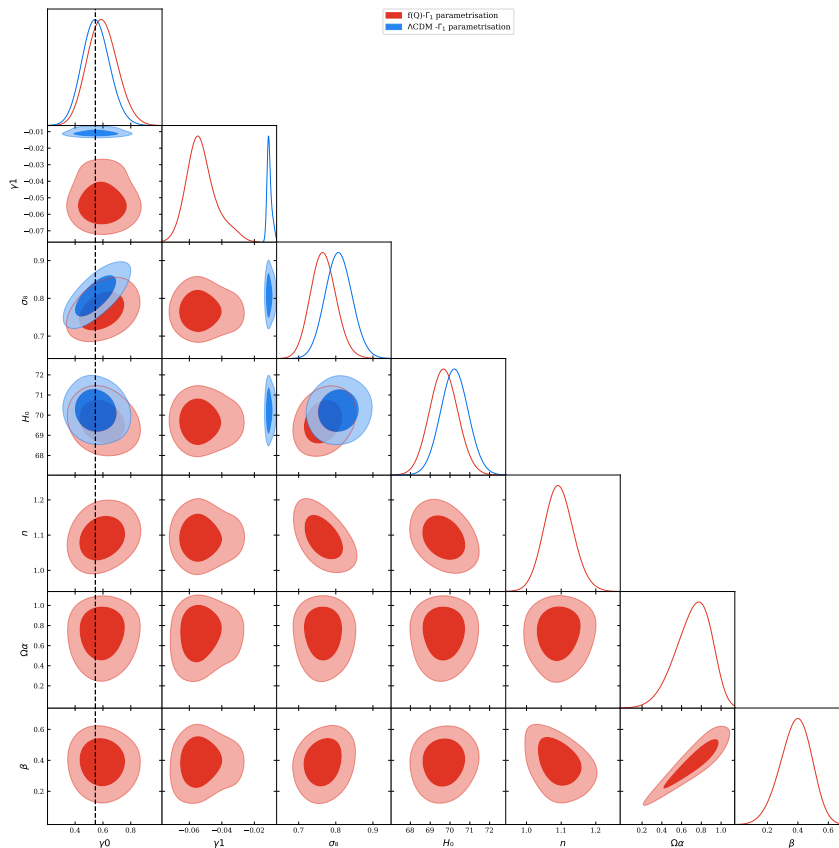


FIG. 2. This figure shows the 1σ and 2σ confidence contours and the posterior distributions obtained from the RSD+CC+Pantheon⁺ datasets for both $f(Q)$ and Λ CDM models using Γ_1 parametrization. The black dashed line represents the theoretical value of $\gamma_0 = 6/11$ for the Λ CDM model.

V. RESULTS AND DISCUSSIONS

In this section, we present the results obtained for Λ CDM and $f(Q)$ gravity models. We constrain the growth index parameters (γ_0, γ_1) of each model using four parameterizations, Γ_{0-3} described previously in the section III, Eqs (3.12), using the following combination of datasets: Pantheon⁺, CC, and RSD. Table IV summarizes the mean values and corresponding errors at the 1σ (68% confidence level, C.L.), while Figs. 1, 2, 3, and 4 depict the confidence contour plots in two dimensions (2D) for the model parameters corresponding to Γ_{0-3} for both models Λ CDM (in blue) and $f(Q)$ gravity (in red). The black dashed lines represent the theoretical value of $\gamma_\Lambda = \frac{6}{11}$ for Λ CDM

In the Λ CDM model, the parameter vector encompasses $\theta_\Lambda = (\Omega_m, \sigma_8, H_0, M, P_\gamma)$, whereas for $f(Q)$ gravity, the parameter vector comprises $\theta_Q = (P_Q, \sigma_8, H_0, M, P_\gamma)$. Notably, for Γ_0 , the associated growth index vector is represented as $P_\gamma \equiv \gamma_0$, while for Γ_{1-3} , it becomes $P_\gamma = (\gamma_0, \gamma_1)$. Additionally, considering the different number of free parameters between the models mentioned above, we employ the Akaike Informa-

tion Criterion (AIC) and Bayesian Information Criterion (BIC), as elaborated in Table V.

A. Constant growth index

1. Γ_0 parametrization model

Firstly, we consider the Γ_0 parametrization ($\gamma = \gamma_0$ and $\gamma_1 = 0$); see Eq. (3.12), which implies that the corresponding statistical vector for the growth index becomes: $P_\gamma \equiv \gamma_0$.

Regarding the Λ CDM model using the Γ_0 parametrization, we find that the growth index $\gamma_0 = 0.545^{+0.096}_{-0.096}$ with $\chi^2_{min} = 1604.15$ for $\mathcal{N}_\Lambda = 5$ degrees of freedom. This result is in good agreement within 1σ errors with those of [105], where they found $\gamma_0 = 0.536^{+0.040}_{-0.018}$ and $\gamma_0 = 0.558^{+0.024}_{-0.018}$ using *ACT*¹+WMAP+BAO and *SPT*²+WMAP+BAO, respectively. It is also

¹ Atacama Cosmology Telescope

² South Pole Telescope

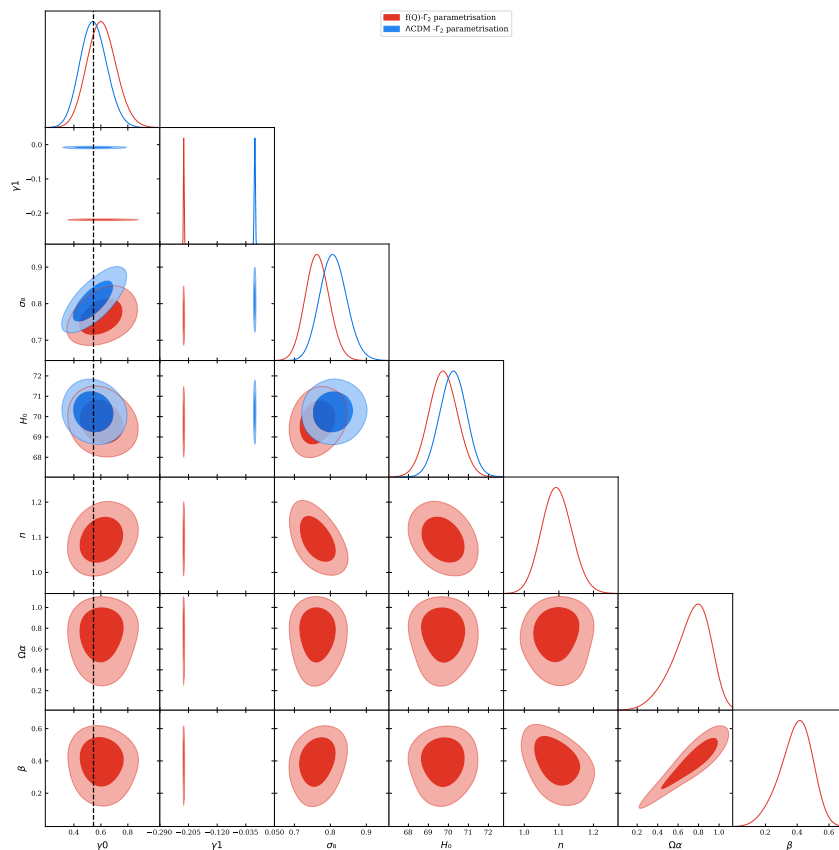


FIG. 3. This figure shows the 1σ and 2σ confidence contours and the posterior distributions obtained from the RSD+CC+Pantheon⁺ datasets for both $f(Q)$ and Λ CDM models using Γ_2 parametrization. The black dashed line represents the theoretical value of $\gamma_0 = 6/11$ for the Λ CDM model.

consistent with [107] within 1σ errors, which found $\gamma_0 = 0.56^{+0.05}_{-0.05}$ using Clustering of *LRGs*³+growth data, and with [40, 41], which found $\gamma_0 = 0.597^{+0.046}_{-0.046}$ using SnIa+BAO+WMAP+CMB+growth dataset. Therefore, the obtained value is in very good agreement with the theoretical value of $\gamma_\Lambda = 6/11$. It becomes evident that we do not restrict any parameter in our present analysis. By employing the most recent growth dataset together with Pantheon⁺ and CC, we can place strong constraints on $\Omega_m = 0.273^{+0.011}_{-0.011}$, $\sigma_8 = 0.808^{+0.0359}_{-0.0359}$, and $H_0 = 70.228^{+0.661}_{-0.661}$, which are also in good agreement with [42].

Regarding the $f(Q)$ expansion model, we find that $\gamma_0 = 0.571^{+0.095}_{-0.110}$ with $\chi^2_{min} = 1599.61$ for $\mathcal{N}_Q = 7$ degrees of freedom. The obtained value of the growth index is somewhat greater than γ_Λ , with differences of 4.66%. Additionally, the cosmological values obtained, $P_Q = (0.72^{+0.22}_{-0.12}, 0.387^{+0.11}_{-0.089}, 1.093^{+0.042}_{-0.042})$, $H_0 = 69.708^{+0.697}_{-0.697}$, and $\sigma_8 = 0.762^{+0.032}_{-0.037}$, are in good

agreement with [42]. A comparison with $f(R)$ and $f(T)$ theories reveals that the growth index of the $f(Q)$ model is lower than that of the Starobinsky $f(R)$ model [41, 106] and the power law $f(T)$ model [40, 108], with differences of 4% and 5.28%, respectively.

Due to the difference in the number of degrees of freedom between Λ CDM and $f(Q)$ ($\mathcal{N}_\Lambda \neq \mathcal{N}_Q$), we compute AIC_c and BIC for both models. The value of $AIC_{c,f(Q)} = 1613.67$ is smaller than the corresponding Λ CDM value $AIC_{c,\Lambda} = 1614.18$, indicating that the $f(Q)$ model, now appears to fit the RSD data slightly better than the usual Λ CDM. However, the small $|\Delta AIC|$ value (i.e., ~ 0.51) points out that Γ_0 parametrization within $f(Q)$ model has substantial support with respect to Λ CDM model. As for ΔBIC (i.e., ~ 10), it reports less evidence against Γ_0 parametrization within $f(Q)$ gravity model.

³ Luminous Red Galaxies

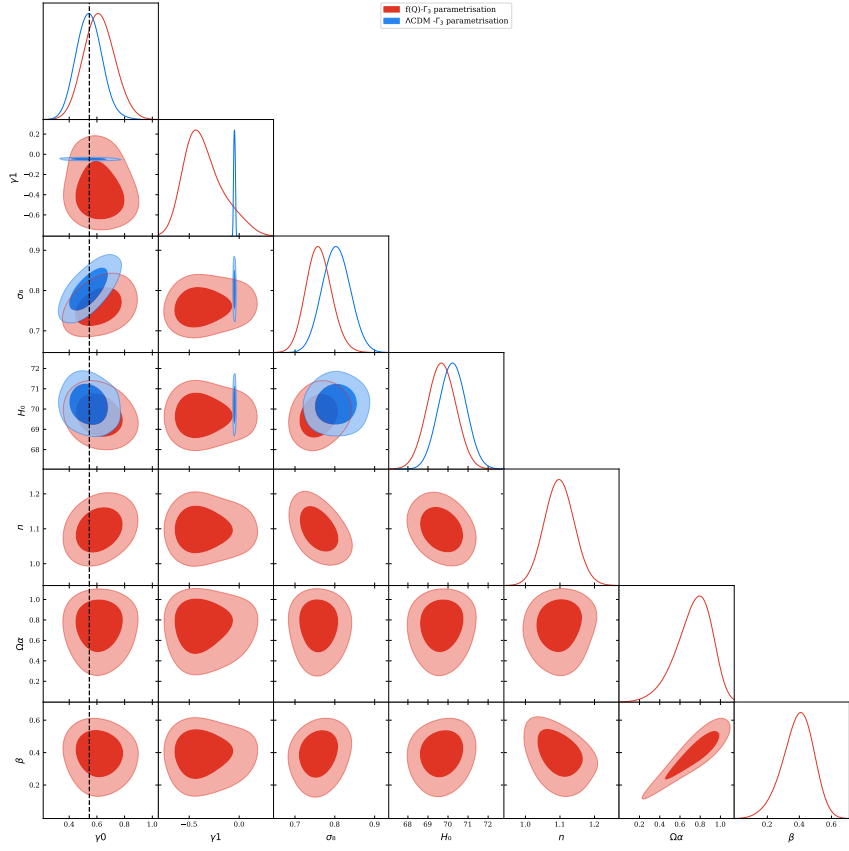


FIG. 4. This figure shows the 1σ and 2σ confidence contours and the posterior distributions obtained from the RSD+CC+Pantheon⁺ datasets for both $f(Q)$ and Λ CDM models using Γ_3 parametrization. The black dashed line represents the theoretical value of $\gamma_0 = 6/11$ for the Λ CDM model.

Model	Parametrization	χ^2_{min}	χ^2_{red}	AIC_c	$ \Delta AIC $	BIC	ΔBIC
Λ CDM	Γ_0	1604.15	0.90476	1614.18	0	1641.57	0
	Γ_1	1604.07	0.90523	1616.12	1.94	1648.97	7.399
	Γ_2	1604.13	0.90526	1616.18	2	1649.03	7.459
	Γ_3	1604.09	0.90524	1616.14	1.96	1641.57	7.419
$f(Q)$	Γ_0	1599.61	0.90322	1613.67	0.51	1651.99	10.423
	Γ_1	1599.55	0.90370	1615.63	1.45	1659.42	17.851
	Γ_2	1599.49	0.90367	1615.57	1.39	1659.36	17.786
	Γ_3	1599.48	0.90366	1615.56	1.38	1659.35	17.779

TABLE V. This table shows values of AIC and BIC for Λ CDM and $f(Q)$ gravity models using Γ_0 , Γ_1 , Γ_2 , and Γ_3 parametrizations.

B. Time varying growth index

After presenting the simplest version of the growth index, Γ_0 , it seems appropriate to discuss the observational constraints on the time-varying growth index, $\gamma(z)$, for the Γ_{1-3} parametrization models. This discussion follows the considerations outlined in section III. Now, the corresponding statistical vector for the growth index becomes $P_\gamma = (\gamma_0, \gamma_1)$.

1. Γ_1 parametrization model

Concerning the Λ CDM model using the Γ_1 parametrization, we find that the growth index parameter results are $\gamma_0 = 0.547^{+0.096}_{-0.096}$ and $\gamma_1 = -0.0106^{+0.0014}_{-0.0014}$, with $\chi^2_{min} = 1604.07$ for $\mathcal{N}_\Lambda = 6$ degrees of freedom. This result is in good agreement within 1σ errors with those of [40, 41], where they found $\gamma_0 = 0.567^{+0.066}_{-0.066}$ and $\gamma_1 = 0.116^{+0.191}_{-0.191}$ using SNIa+BAO+WMAP+CMB+growth dataset.

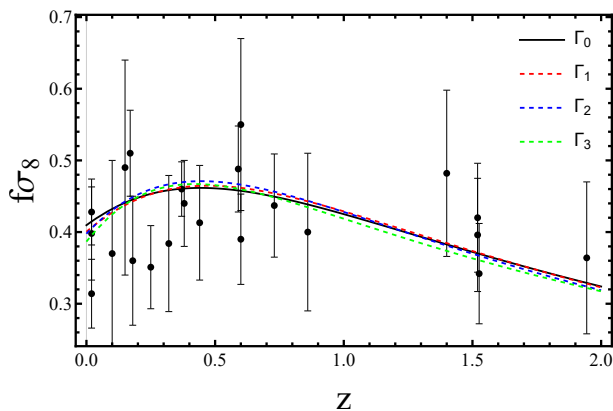


FIG. 5. This figure shows the evolution of the predicted $f\sigma_8$ observable versus the redshift, z . The results given by the models Γ_0 (in black), Γ_1 (red dashed), Γ_2 (blue dashed), and Γ_3 (green dashed) in $f(Q)$ gravity.

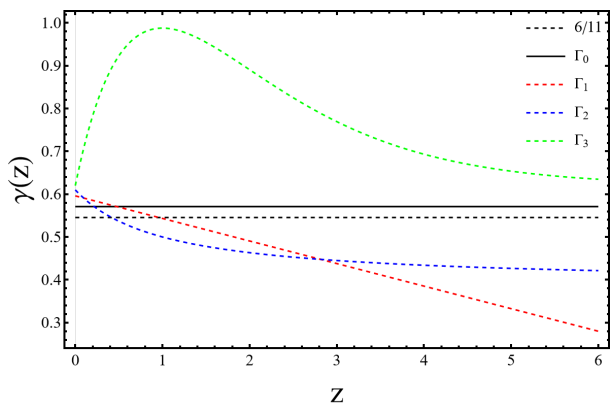


FIG. 6. The evolution of the growth index function γ versus redshift, z , for parametrization models Γ_0 (in black), Γ_1 (red dashed), Γ_2 (blue dashed), and Γ_3 (green dashed) in $f(Q)$ gravity. The black dashed line represents the theoretical value $\gamma_\Lambda = 6/11$ of the Λ CDM model.

Concerning the $f(Q)$ model, we find that $\gamma_0 = 0.596^{+0.097}_{-0.11}$ and $\gamma_1 = -0.0527^{+0.0057}_{-0.0098}$, with $\chi^2_{min} = 1599.55$ for $\mathcal{N}_Q = 8$ degrees of freedom. The obtained γ_0 value is greater than γ_Λ by a difference of 9%. A comparison between $f(R)$ and $f(T)$ theories indicates that the growth index of the $f(Q)$ model is greater than that of both the Starobinsky $f(R)$ model [41, 106] and the power law $f(T)$ model [40, 108], with differences of 5% and 6.58%, respectively.

We notice that the value of $AIC_{c,f(Q)} = 1615.63$ is smaller than the corresponding Λ CDM value $AIC_{c,\Lambda} = 1616.12$, indicating that the $f(Q)$ model appears to fit slightly better than the usual Λ CDM. However, the small $|\Delta AIC|$ value (i.e., ~ 1.45) indicates that Γ_1 parametrization within the studied $f(Q)$ model has substantial support with respect to Λ CDM. In the other hand, the value of $\Delta BIC = 17.851$ reports strong ev-

idence against Γ_1 parametrization within $f(Q)$ gravity model.

2. Γ_2 parametrization model

Regarding the Λ CDM model using the Γ_2 parametrization, we find that the growth index parameters are $\gamma_0 = 0.544^{+0.097}_{-0.097}$ and $\gamma_1 = -0.00827^{+0.00154}_{-0.00154}$, with $\chi^2_{min} = 1604.13$ for $\mathcal{N}_\Lambda = 6$ degrees of freedom. This result is in good agreement within 1σ errors with those of [40, 41], where the authors found $\gamma_0 = 0.561^{+0.068}_{-0.068}$ and $\gamma_1 = 0.183^{+0.269}_{-0.269}$ using SnIa+BAO+WMAP+CMB+growth dataset. Additionally, it is within 1σ errors of the results of [109], where the authors found $(\gamma_0, \gamma_1) \simeq (0.557, -0.012)$ using SnIa+BAO+CMB+Big Bang Nucleosynthesis+ $H(z)$ +growth index dataset.

While in the $f(Q)$ model, we find that $\gamma_0 = 0.544^{+0.097}_{-0.097}$ and $\gamma_1 = -0.0527^{+0.0057}_{-0.0098}$, with $\chi^2_{min} = 1599.49$ for $\mathcal{N}_Q = 8$ degrees of freedom. The obtained γ_0 value is greater than γ_Λ with differences of 9%. When comparing the growth index of $f(R)$ and $f(T)$ theories with that of $f(Q)$, it becomes evident that the growth index of the $f(Q)$ model surpasses both the Starobinsky $f(R)$ [41, 106] and the power law $f(T)$ models [40, 108], exhibiting differences of 8.36%.

We notice that the value of $AIC_{c,f(Q)} = 1615.57$ is smaller than the corresponding Λ CDM value $AIC_{c,\Lambda} = 1616.18$, indicating that the $f(Q)$ model appears to fit slightly better than the usual Λ CDM. However, the small $|\Delta AIC|$ value (i.e., ~ 1.39) indicates that the Γ_1 parametrization within the studied $f(Q)$ model has substantial support with respect to Λ CDM. In the other hand, the value of $\Delta BIC = 17.886$ reports a strong evidence against Γ_2 parametrization within $f(Q)$ gravity model.

3. Γ_3 parametrization model

In the context of the Γ_3 parametrization, concerning the Λ CDM model, we find that the growth index parameters are $\gamma_0 = 0.542^{+0.092}_{-0.092}$ and $\gamma_1 = -0.047^{+0.007}_{-0.007}$, with $\chi^2_{min} = 1604.09$ for $\mathcal{N}_\Lambda = 6$ degrees of freedom. Meanwhile, in the $f(Q)$ model, we find that $\gamma_0 = 0.62^{+0.10}_{-0.12}$ and $\gamma_1 = -0.359^{+0.093}_{-0.24}$, with $\chi^2_{min} = 1615.56$ for $\mathcal{N}_Q = 8$ degrees of freedom. The obtained γ_0 value is greater than γ_Λ by approximately 9%.

As observed in previous Γ_0 , Γ_1 , and Γ_2 models, the value of $AIC_{c,f(Q)} = 1599.48$ is also smaller than the corresponding Λ CDM value $AIC_{c,\Lambda} = 1604.09$, indicating that the $f(Q)$ model appears to fit slightly better than the usual Λ CDM. However, the small $|\Delta AIC|$ value

(i.e., ~ 1.38) indicates that the Γ_3 parametrization within the studied $f(Q)$ model has substantial support with respect to Λ CDM. In the other hand, the value of $\Delta BIC = 17.78$ points out to a strong evidence against Γ_3 parametrization within $f(Q)$ gravity model.

Let's delve into the cosmic evolution of the growth factor, $f\sigma_8(z)$, and the growth index, $\gamma(z)$, across various parametrization models, Γ_{0-3} , within the context of $f(Q)$ gravity. Our aim is to analyze and quantify their evolution as defined by Eqs. (3.2) and (3.12). Fig. 5 illustrates the predicted evolution of $f\sigma_8$ using the mean values of P_Q and P_γ obtained previously from RSD data combined with Pantheon⁺ and CC. (Table IV). Notably, the predictions clearly align with the RSD measurements, indicating the effectiveness of each parametrization model. Therefore, Fig. 6 depicts the evolution of $\gamma(z)$, where the dashed black line represents the prediction of the Λ CDM model. Remarkably, for Γ_0 , the growth index remains constant throughout the entire range $z \sim 0-6$. However, Γ_1 and Γ_2 exhibit medium deviations from the growth index γ_Λ , whereas Γ_3 displays significant deviations within the range of $z \sim 0.5-3$.

VI. CONCLUSION

It is widely acknowledged that the growth index, γ , plays a key role in understanding the formation and evolution of large-scale structures over time. Moreover, it serves as a valuable tool for testing theories of gravity, such as Einstein's general relativity. In this work, we have used recent observational data, including Pantheon⁺, cosmic chronometer, and redshift space distortion datasets, to constrain the parameters of the

growth index within the framework of $f(Q)$ gravity. Our aim was twofold: first, apply a Markov Chain Monte Carlo analysis across various γ parametrization models within the context of $f(Q)$ gravity, and second, to quantify the deviation between our $f(Q)$ and the standard Λ CDM models.

Initially, we have explored a constant growth index parametrization, $f(z) = \Omega_m(z)^\gamma$, where $\gamma = \gamma_0$. For Λ CDM, our analysis revealed that the observed growth index $\gamma_0 = 0.545 \pm 0.096$ aligns well, within 1σ errors, with results from various previous studies, such as [40, 41, 105, 107]. Moreover, it is in very good agreement with the theoretically predicted value of $\gamma_\Lambda = 11/6$. However, for the $f(Q)$ model, we have found a deviation of 4.66% from the Λ CDM model, with the value of the growth index $\gamma_0 = 0.571_{-0.110}^{+0.095}$.

Subsequently, we have considered a time-varying growth index parametrization, $f(z) = \Omega_m(z)^{\gamma(z)}$, with $\gamma(z) = \gamma_0 + \gamma_1 y(z)$, where $y(z) = z, 1 - 1/(1+z)$, and ze^{-z} . We have found that $(\gamma_0, \gamma_1) = (0.596, -0.0527)$, $(\gamma_0, \gamma_1) = (0.61, -0.22)$, and $(\gamma_0, \gamma_1) = (0.62, -0.359)$, for Γ_1 , Γ_2 , and Γ_3 models, respectively. However, we have found that the γ_0 values for the Γ_{1-3} parametrization models are greater than that of Λ CDM by a difference of 9%.

Finally, an examination of the evolution of the growth index $\gamma(z)$ versus redshift z for each parametrization model revealed distinct behaviors. While Γ_0 maintained constancy across the entire range $z \sim 0-6$, Γ_1 and Γ_2 exhibit medium deviations from the growth index γ_Λ , whereas Γ_3 displays significant deviations within the range of $z \sim 0.5-3$.

-
- [1] Z.Y. Huang et al., J. Cosmol. Astropart. Phys. 0605, 013 (2006).
 - [2] E. Komatsu et al., Astrophys. J. Suppl. 192, 18 (2011).
 - [3] T. Koivisto, D.F. Mota, Phys. Rev. D 73, 083502 (2006).
 - [4] S.F. Daniel, Phys. Rev. D 77, 103513 (2008).
 - [5] A.G. Riess et al., Astron. J. 116, 1009 (1998).
 - [6] S. Perlmutter et al., Astrophys. J. 517, 377 (1999).
 - [7] A.G. Riess et al., Astrophys. J. 607, 665 (2004).
 - [8] V. Sahni, A. Starobinsky, Internat. J. Modern. Phys. D 9, 373 (2000).
 - [9] P.J.E. Peebles, B. Ratra, Rev. Mod. Phys. 75, 559 (2003).
 - [10] N. Sivanandam, Phys. Rev. D 87, 083514 (2013).
 - [11] H.E. Velten et al., Eur. Phys. J. C 74, 1 (2014).
 - [12] E. Di Valentino, et al., Classical and Quantum Gravity, 38(15), 153001, (2021).
 - [13] S. Dahmani et al., Physics of the Dark Universe, 101266(2023)
 - [14] S. Dahmani et al., General Relativity and Gravitation 55, 22 (2023).
 - [15] J. Martin, Modern Physics Letters A 23, 1252 (2008)
 - [16] Y. Ladghami et al., Annals of Physics 460, 169575 (2024)
 - [17] A. Bouali et al., Physics of the Dark Universe 34, 100907(2021)
 - [18] D. Mhamdi et al., Gen. Relativ. Gravit. 55, 11 (2023)
 - [19] M.-H. Belkacemi et al., International Journal of Modern Physics D 29, 2050066 (2020).
 - [20] F. Bargach et al., International Journal of Modern Physics D 30, 2150076 (2021).
 - [21] M. Bouhmadi-López et al., The European Physical Journal C, 78, 1-11, (2018).
 - [22] S. Sen et al., Physical Review D 63, 124006 (2001).
 - [23] A. Errahmani, T. Ouali, Modern Physics Letters A, 23, 3095-3111, (2008).
 - [24] A. Errahmani, T. Ouali, Physics Letters B, 641, 357-361, (2006).
 - [25] A. De Felice & S. Tsujikawa. Living Reviews in Relativity, 13(1), 1-161, (2010).
 - [26] H.A. Buchdahl, Mon. Notices Royal Astron. Soc. 150, 1 (1970).
 - [27] J. B. Jiménez et al., Phys. Rev. D 101, 103507 (2020).

- [28] F. Bajardi et al., *Eur. Phys. J. Plus*, 135, 912 (2020).
- [29] K. Flathmann, & M. Hohmann, *Phys. Rev. D*, 103, 044030 (2021).
- [30] F. D'Ambrosio et al., *L. Phys. Lett. B*, 811, 135970 (2020).
- [31] L. Heisenberg, *Physics Reports*, 1066, 1-78 (2024).
- [32] N. Frusciante, *Phys. Rev. D*, 103, 044021 (2021).
- [33] S. Mandal, & P. K. Sahoo. *Phys. Lett. B*, 823, 136786 (2021).
- [34] F. K Anagnostopoulos et al., *Phys. Lett. B*, 822 (2021).
- [35] B. J. Barros et al., *Phys. Dark Univ.*, 30, 100616 (2020).
- [36] M. Koussour et al., *Fortschritte der Physik*, 71(4-5), 2200172 (2023).
- [37] I. Ayuso et al., *Phys. Rev. D*, 103, 063505 (2021).
- [38] W. Khyllap et al., *Phys. Rev. D*, 103, 103521 (2021).
- [39] S. Capozziello et al., *Phys. Lett. B*, 832, 137229 (2022).
- [40] S. Nesseris et al., *L. Phys. Rev. D*, 88(10), 103010 (2013).
- [41] S. Basilakos et al., *L. Phys. Rev. D*, 87(12), 123529 (2013).
- [42] D. Mhamdi et al., *Eur. Phys. J. C* 84, 310 (2024).
- [43] H. Akaike, *IEEE transactions on automatic control*. 19, 716–723 (1974).
- [44] A. R. Liddle, *MNRAS*. 377 L74–L78 (2007).
- [45] G. Schwarz, *Ann. Stat.* 6 461 (1978).
- [46] J. B. Jiménez et al., *Phys. Rev. D* 98, 044048 (2018).
- [47] G. G. L. Nashed, *Fortschritte der Physik*, 2400037 (2024).
- [48] R. Dave et al., *Phys. Rev. D*, 66, 023516 (2002).
- [49] R. Gannouji et al., *JCAP*, 62, 034 (2009).
- [50] P. J. Uzan, *Gen. Rel. Grav.*, 39, 307 (2007).
- [51] F. H. Stabenau and B. Jain, *Phys. Rev. D*, 74, 084007 (2006).
- [52] P. J. E. Peebles, *Principles of Physical Cosmology*, Princeton University Press, Princeton New Jersey (1993).
- [53] A. Lue et al., *Phys. Rev. D*, 69, 124015 (2004).
- [54] V. Silveira and I. Waga, *Phys. Rev. D*, 50, 4890 (1994).
- [55] L. Wang and J. P. Steinhardt, *Astrophys. J*, 508, 483 (1998).
- [56] S. Nesseris and L. Perivolaropoulos, *Phys. Rev. D* 77, 023504 (2008).
- [57] S. Tsujikawa et al., *Phys. Rev. D*, 80, 084044 (2009).
- [58] D. Polarski and R. Gannouji, *Phys. Lett. B* 660, 439 (2008).
- [59] A. B. Belloso et al., *JCAP*, 1110, 010 (2011).
- [60] M. Ishak and J. Dosset, *Phys. Rev. D*, 80, 043004 (2009).
- [61] C. Di Porto et al., *Mon. Not. Roy. Astron. Soc.* 419, 985 (2012).
- [62] S. Basilakos & A. Pouri, *Mon. Not. Roy. Astron. Soc.* 423(4), 3761-3767 (2012).
- [63] A. Mehrabi et al., *MNRAS* 452, 2930 (2015).
- [64] A. Lewis et al., *Phys. Rev. D* 66, 103511 (2002).
- [65] W. R. Gilks et al., *Markov chain monte carlo in practice* (CRC Press, London, 1995)
- [66] A. Lewis, arXiv preprint arXiv:1910.13970 (2019).
- [67] D. Brout et al., *ApJ* 938, 2 (2022)
- [68] C. H. Chuang et al., *Mon. Not. Roy. Astron. Soc.*, 435, 255–262 (2013).
- [69] J. E. Bautista et al., *Astron. Astrophys.*, 603, A12, 23pp (2017).
- [70] A. Oka et al., *Mon. Not. Roy. Astron. Soc.*, 439, 2515–2530 (2014).
- [71] J. Simon et al., *Phys. Rev. D*, 71, 123001 (2005).
- [72] A. L. Ratsimbazafy et al., *Mon. Not. Roy. Astron. Soc.*, 467, 3239–3254 (2017).
- [73] C. Zhang et al., *Research in Astron. and Astrop.*, 14, 1221-1233 (2014).
- [74] J. Simon et al., *Phys. Rev. D*, 71, 123001 (2005).
- [75] M. Moresco et al., *J. Cosmol. Astropart. Phys.*, 8, 006 (2012).
- [76] M. Moresco et al., *J. Cosmol. Astropart. Phys.*, 05, 014 (2016).
- [77] A. Ratsimbazafy et al., *Mon. Not. Roy. Astron. Soc.*, 467, 3239–3254 (2017).
- [78] D. Stern et al., *J. Cosmol. Astropart. Phys.*, 02, 008 (2010).
- [79] M. Moresco et al., *J. Cosmol. Astropart. Phys.*, 8, 006pp (2012).
- [80] M. Moresco et al., *Mon. Not. Roy. Astron. Soc.: Letters*, 450, L16-L20 (2015).
- [81] Gaztañaga et al., *Mon. Not. Roy. Astron. Soc.*, 399, 1663–1680.
- [82] Y. Wang et al., *Mon. Not. Roy. Astron. Soc.*, 469, 3762–3774 (2017).
- [83] C. H. Chuang, & Y. Wang, *Mon. Not. Roy. Astron. Soc.*, 435, 255–262. (2013)
- [84] C. Blake et al., *Mon. Not. Roy. Astron. Soc.*, 425, 405–414 (2012).
- [85] S. Alam et al., *Mon. Not. Roy. Astron. Soc.*, 470, 2617–2652 (2017).
- [86] C. H. Chuang et al., *Mon. Not. Roy. Astron. Soc.*, 433, 3559–3571 (2013).
- [87] T. Delubac et al., *Astron. Astrophys.*, 574, A59 (2015).
- [88] L. Anderson et al., *Mon. Not. Roy. Astron. Soc.*, 441, 24pp (2014).
- [89] A. Font-Ribera et al., *J. Cosmol. Astropart. Phys.*, 05, 027 (2014).
- [90] N. G. Busca et al., *Astron. and Astrop.*, 552, A96 (2013).
- [91] J. E. Bautista et al., *Astron. Astrophys.*, 603, A12, 23pp (2017).
- [92] S. J. Turnbull et al., *MNRAS* 420, 447 (2012), 1111.0631.
- [93] I. Achitouv et al., *Phys. Rev. D* 95, 083502 (2017), 1606.03092.
- [94] F. Beutler et al., *MNRAS* 423, 3430 (2012), 1204.4725.
- [95] M. Feix et al., *Phys. Rev. Lett.* 115, 011301 (2015), 1503.05945.
- [96] S. Alam et al., *MNRAS* 470, 2617 (2017), 1607.03155.
- [97] A. G. Sánchez et al., *MNRAS* 440, 2692 (2014), 1312.4854.
- [98] C. Blake et al., *MNRAS* 425, 405 (2012), 1204.3674.
- [99] S. Nadathur et al., *Phys. Rev. D* 100, 023504 (2019), 1904.01030
- [100] C.-H. Chuang et al., *MNRAS* 461, 3781 (2016),
- [101] M. Aubert et al., arXiv e-prints, arXiv:2007.09013 (2020), 2007.09013.
- [102] M. J. Wilson, arXiv e-prints, arXiv:1610.08362 (2016), 1610.08362.
- [103] G.-B. Zhao et al., *MNRAS* 482, 3497 (2019), 1801.03043.
- [104] T. Okumura et al., *PASJ* 68, 38 (2016).
- [105] E. Specogna et al., *Physical Review D*, 109(4), 043528 (2024),
- [106] A. A. Starobinsky, *JETP Lett.* 86, 157 (2007)
- [107] A. Pouri et al., *J. Cosmol. Astropart. Phys.*, 08, 042

- (2014).
- [108] G. R. Bengochea, & R. Ferraro, Phys. Rev. D, 79, 124019, (2009).
- [109] A. Mehrabi et al., Physical Review D, 92(12), 123513 (2015).